Electrical Characteristics of Parallel-Plate RF Discharges in Argon

Valery A. Godyak, *Member, IEEE*, Robert B. Piejak, and Benjamin M. Alexandrovich

Abstract— **Electrical characteristics have been measured in a parallel-plate, capacitively coupled (E-type), low-pressure, symmetrical RF discharge driven at 13.56 MHz. The discharge voltage, current, and phase shift between them were measured over a very wide range of discharge parameters (gas pressures between 3 mtorr and 3 torr with discharge power between 20 mW and 100 W). From these measurements the discharge impedance components, the power dissipated in the plasma and in the sheaths, the sheath width, and the ion current to the RF electrodes were found over a wide range of discharge conditions. Some of the general relationships between the various measured and determined parameters are discussed. The experimental results presented here can be used as a data base for straightforward comparison with existing RF discharge models and numerical simulations.**

I. Introduction

RADIO-FREQUENCY (RF) discharges are of great importance and interest in a variety of applications, among which plasma processing technology is the best known. Quite a few approaches have been developed to model the characteristics of RF discharges. Unfortunately and mysteriously, no comparisons of these models with each other can be found in the literature. More importantly, there are no comparisons of these models with experimental data, probably due to the absence of accurate and systematic measurements of discharge parameters over a comprehensive range of gas pressure and discharge power.

Some measurements of various electrical parameters in RF discharges can be found in the literature [1]–[10]; however, to our knowledge most measurements are not of great use for making general conclusions about scaling laws or for verifying existing models because of a variety of reasons:

a) There is an absence of complete, accurate, and systematic measurements of the discharge electrical characteristics over a comprehensive range of gas pressure and discharge power. Various discharge characteristics have been measured, but under differing discharge conditions (gas type, pressure, electrode gap, discharge power, etc.) and in different reactors. This makes it impossible to put results obtained by different experimentalists together to achieve a complete discharge characterization.

b) In many cases, the measurements are made over a range of parameter space too limited to establish scaling laws for the discharge parameters. Although the models may indeed be in agreement at a specific point, there is insufficient data to show if the models can accurately predict operating conditions at widely ranging points. Without such comparisons, it is impossible to employ these models confidently in a predictive (rather than a confirmative) mode.

c) Many measurements characterize the discharge as a function of RF power transmitted to the matcher located between a power meter and the discharge reactor, assuming the matching network to be a lossless impedance transformer. Although easy to do, this method may be in serious error due to matcher losses that can account for up to 90% of the measured transmitted power. Since the fraction of matcher network losses varies with loading (which varies widely), estimating the discharge power to be proportional to the transmitted power could also be in error. Furthermore, discharge characterization by the discharge power seems to be not very useful, primarily because discharge power is not a fundamental gas discharge parameter, and thus relationships between physical processes and fundamental discharge properties may be obscured by this representation.

d) Many experiments have an inherent incompatibility with one-dimensional discharge concepts and discharge models due to asymmetry of the discharge. Most models assume discharge symmetry, while most experiments are driven asymmetrically and often have unequal electrode areas for RF current flow.

e) In some experiments the discharge volume varies considerably and is not determinable. In many measurements within reactors where the discharge is not confined radially, the plasma volume varies with power, gas pressure, and gas type and does not necessarily conform to observed discharge brightness.

f) Less than optimum measurement accuracy also occurs in systems which must be partially disassembled to make measurements. The problem here is that the contact resistances at the points of assembly change unpredictably after assembly and disassembly.

g) Finally, there are systems which are simply unsuitable for direct electrical measurements. Because of their physical layout it is virtually impossible to attain high accuracy, since measurements cannot be made directly across the discharge. When there is appreciable series and/or shunt impedance between the measurement points and discharge, it becomes difficult to ascertain with high accuracy the discharge voltage and current, even if values of the layouts' reactive elements can be determined. The difficulty is a fundamental problem; i. e., determining with reasonable accuracy a high impedance element in parallel with a low impedance element, or a low impedance element in series with a high impedance element.

Manuscript received February 12, 1991; revised April 10, 1991.
The authors are with GTE Laboratories Incorporated, Waltham MA 02254.
IEEE Log Number 9101104.

There are further complications with this approach due to frequency dependence of the stray reactance and resistive losses that always appear in practical situations. This problem may be compounded in reactors with asymmetric discharges where the content of higher harmonics is considerably greater.

In this work we have (hopefully) avoided these difficulties by designing an experimental system not as a prototype of a processing device but as a discharge physics research chamber. To do this, two basic principles were put into the design of this experimental system—first, well-defined and simple discharge geometry was used to insure overall discharge symmetry, i.e., to make the discharge compatible (as much as possible) with one-dimensional models; and secondly, the discharge layout (shape, geometry) was designed to facilitate discharge and plasma parameter diagnostics, i.e., adjusting the discharge to the diagnostics, not the diagnostics to the discharge! Following this approach, we have chosen a radially confined symmetrically (push–pull) driven parallel-plate RF discharge with equal area electrodes.

This approach drastically reduces the harmonic content of the system and has the following important consequences: the RF discharge can be considered over an RF period as a linear device; i.e., having a nearly linear dynamic current/voltage characteristic (although the discharge is predominantly reactive in impedance and nonlinear in terms of its static current/voltage characteristic). This allows one unambiguously to characterize the discharge by the equivalent series resistance R and capacitance C (both being functions of discharge conditions determined at the fundamental frequency only). Aside from a reduction in harmonics, the discharge symmetry also results in an order of magnitude reduction in the plasma RF potential with respect to the ground. This significantly reduces the radial RF current which is proportional to the RF plasma potential and plasma capacitance to the ground. Thus the radial current can be made negligible compared to the measured axial RF current, thereby contributing to the one-dimensional character of the discharge. Another advantage of reducing the RF plasma potential is to facilitate Langmuir probe diagnostics in the RF plasma. And finally, the balanced symmetric discharge excitation practically eliminates RF interference with nearby electronic equipment and problems associated with ground loops.

Electrically, RF discharges with negligible harmonic content can be fully characterized by pairs of functions $V(I)$ and $P(I)$ or $R(P)$ and $X(P)$, where the discharge scalar parameters are: voltage (amplitude) V, current (amplitude) I, rms power P, reactance X, and resistance R. The phase shift ϕ or power factor $\cos\phi$ can be readily found from the expression:

$$\cos\phi = 2P/IV = (1 + X^2/R^2)^{-1/2}.$$

We have chosen discharge voltage and current as primary discharge parameters. Together with phase shift or discharge power, these parameters completely define discharge conditions. This manner of characterization is convenient and informative in terms of gas discharge physics, since current and voltage are integrals of two fundamental discharge parameters; namely, the current density and electric field. All the aforementioned electrical parameters are coupled through the simple expressions:

$$P = 1/2 \cdot IV\cos\phi; \qquad R = (V/I)\cdot\cos\phi;$$
$$X = (V/I)\cdot\sin\phi.$$

In this work the discharge current, voltage, and phase shift between them were measured in a symmetrically driven, parallel-plate, argon RF discharge at 13.56 MHz. The measurements have been made over a wide range of gas pressure (3 mtorr–3 torr) and discharge power (20 mW–100 W). Over this range of gas pressure the electron-heating mechanism changes from a stochastically dominated to a collisionally dominated one, while over this range of power, RF power deposition changes from mainly into the plasma electrons to mainly into the ions in the electrode sheaths.

From these measurements, discharge power and the series equivalent discharge resistance and capacitance have been found. Experimental scaling laws for discharge electrical parameters allowed us to find the power share between the plasma electron heating and ion acceleration in the electrode sheaths, the RF sheath voltage, the ion current to the electrodes, and the sheath width over a wide range of discharge conditions. The results presented here can be used as a data base for verifying existing RF discharge theories and numerical simulation experiments.

II. Experimental System

A schematic diagram of the electrical measurement setup is shown in Fig. 1. The entire experimental system has been described elsewhere [11], [12], so only a cursory description related to the electrical characteristic measurements will be given here. The discharge gap is formed by two parallel-plate aluminum electrodes separated by a distance L = 6.7 cm. The discharge separation was chosen to be large enough that "collisionless" discharges at pressures as low as 3 mtorr could be studied without overlapping electrode sheaths, and to be small enough that it could be considered as one-dimensional. A glass cylinder with an inner diameter of 14.3 cm (cross section A = 160 cm^2) confines the discharge radially and is easily accessible for diagnostic study. Having transparent glass walls, one can easily observe the electrode sheaths, the plasma body shape, and any changes in the discharge luminosity which might accompany transitions in discharge regimes and discharge instabilities. Wire probes are mounted in the medial plane of the discharge to measure internal plasma parameters [13] and the dc and RF plasma potential [14].

During operation, argon gas (99.998% min. purity) is flowed through the discharge chamber to maintain gas purity. The background pressure in the vacuum chamber is in the 10^{-8} torr range and presumably is an order of magnitude higher in the discharge chamber. The leak rate has been measured to be less than 2×10^{-5} sccm. Gas purity in the discharge is better than 99.95% at the worst case of p = 3 mtorr when the flow rate (0.1 sccm) is limited by the conductivity of the connecting tube between the discharge and vacuum chambers. At higher gas pressure, the flow rate is larger and maintained at 20 sccm. No dependency was observed in the measured electrical characteristics versus flow rate when the flow rate

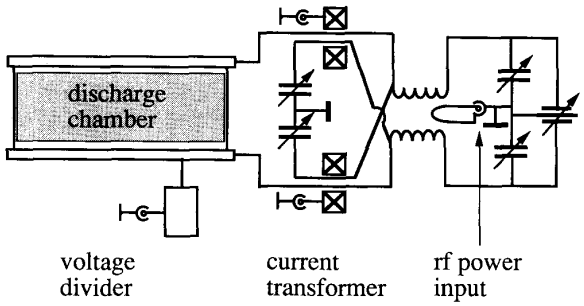

Fig. 1. A schematic diagram of the electrical measurement setup.

was changed by 20 times at low gas pressure ($p < 0.5$ torr). For high gas pressure $p > 0.5$ torr, a small (within 5%) change in cos ϕ was found when gas flow was changed from 1 to 200 sccm, while no changes were found in RF voltage and current values over the full range of discharge power.

Power to the discharge is provided by a wideband RF amplifier. It is fed through a directional coupler into a matching system which is directly connected to the discharge electrodes. The electrodes are driven "push–pull" to create an electrically symmetric discharge with respect to ground. The RF voltage across the electrodes is measured through a voltage divider directly connected to each electrode. Connecting voltage dividers directly to the electrodes eliminates the voltage drop across the contacts and across the inductance of the power supply leads. Before recording data, the symmetry of the matcher is adjusted so that the voltage applied to each electrode is equal (but opposite in phase). Typically, voltage is measured at one electrode, and this voltage is doubled to determine the total voltage between electrodes. The symmetry in the applied voltage is monitored by a capacitive probe (a 0.6 × 2.0 cm strip of copper foil placed on the external glass wall in the discharge midplane). The absence of fundamental harmonic in the probe signal appears to be a sensitive indicator of discharge symmetry.

Discharge current is measured with miniature current transformers (CT's) in each lead of the discharge only a few centimeters back from where the matcher connects to the electrodes. Current measurements are compensated to eliminate fringe and stray capacitance and the symmetry is checked and reset if necessary before making measurements. For symmetrically driven discharges, the ratio between the radial current I_r and the measured axial discharge currents I is estimated to be: $I_r/I \approx 5\ dS_0/A$, where d is the plasma half-width, S_0 is the RF sheath width, and A is the discharge cross section. Over all conditions of this experiment, I/I_r was less than 0.1 at the worst case.

Current measurements are made with both CT's connected in parallel such that small changes in symmetry during discharge operation do not affect overall phase measurements. Direct measurement of the voltage and current as described here is a straight-forward embodiment of the well-known four-wire technique.

Both the RF voltage and current are measured with two-channel digital RF millivoltmeter having a base accuracy of 1% and factory-calibrated current transformers and voltage dividers with an accuracy of 1%. Based on the measuring system calibration with known dummy loads and the reproducibility of the many results obtained over a one-year period [11], we estimate that the real accuracy in the voltage and current measurements presented in this paper is within 5%.

Phase measurements between discharge current and voltage were accurately measured with a network analyzer. Prior to measurements with an RF discharge, a high Q-factor capacitor approximately equal to the equivalent capacitance of the discharge was tied across the electrodes, and the network analyzer was calibrated to indicate a 90° phase shift. The calibration was generally done with the discharge chamber at minimum gas pressure (10^{-7} torr range), and the voltage applied to the electrodes was kept below 50 V rms to prevent exciting a multipacting (dark) discharge and thus introducing unwanted conductivity between the electrodes. In previous work [12], a waveform analyzer was used to determine the phase shift; however, we have found that the network analyzer is very accurate and is substantially faster to use. The phase measurement accuracy, which is critical for power calculation in highly reactive RF discharges, is estimated to be within 0.1°, which corresponds to a power factor (cos ϕ) error of no greater than 5%. More details about the experimental system can be found in [11] and [12].

Wherever possible, discharge current measurements were made between a few milliamperes and a few amperes. The discharge voltage was varied between 10 V to greater than 1 kV. In most cases, the upper current limit of the discharge was set by the power limitation of the RF amplifier, but in a few cases the discharge current was limited by the occurrence of anomalous discharges (to ground via the gas flow tubes), which spoiled the discharge symmetry and introduced harmonics. The lower limit on discharge current was close to the discharge extinction where the RF sheath started to grow and the plasma body shrunk, forming an oblate spheroid shaped plasmoid. For all cases voltage waveforms were sinusoidal, while the current waveforms manifested just a few percent in harmonic content (only at higher discharge current). A typical oscillogram of the discharge voltage, current, and RF plasma potential is shown in Fig. 2. Results from the measurements of the RF and dc plasma potential and measurements of ion current to the RF electrode are in [14] and [15], respectively. Throughout this paper the values of RF currents and voltages are given in terms of amplitude.

III. Experimental Results and Discussion

A. Power Factor

Typical behavior of the discharge power factor (cos ϕ) is presented as a function of discharge current in Fig. 3(a), and as a function of discharge voltage in Fig. 3(b). For all discharge conditions, the phase shift ϕ was found to correspond to a capacitive (negative reactance) RF discharge impedance. cos ϕ increased with decreasing discharge current and/or increasing gas pressure and ultimately approaches unity (cos $\phi = 1$). At high discharge current and voltage, cos ϕ reached a minimum

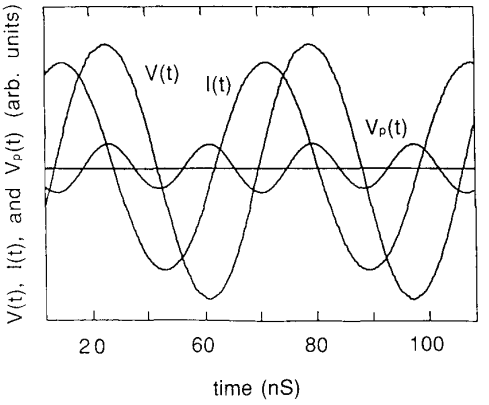

Fig. 2. Oscillograms of the discharge voltage $V(t)$, discharge current $I(t)$, and the RF plasma potential $V_p(t)$ at the midplane of the discharge at 1 torr in argon. The amplitudes of these waveforms are 140 V, 1 A, and 11.3 V, respectively.

followed by a slow rise with increasing current. General features in the behavior of $\cos\phi$ are $\cos\phi \propto V^{-1}$ at small discharge current, and $\cos\phi \approx$ constant at large discharge current. This results in the following consequences: the ohmic component of the discharge voltage $V\cos\phi$ is nearly constant at small discharge current and is proportional to V (discharge resistance $R \approx$ constant) at large discharge current.

B. Voltage and Power

The current/voltage $V(I)$ characteristics and current/power $P(I)$ characteristics of the RF discharge are given in Figs. 4(a)–(d) and 5(a)-(d) for 8 gas pressures between 3 mtorr and 3 torr. Current and voltage were measured directly together with the phase shift ϕ between them; discharge power was computed as $P = 1/2 \cdot IV\cos\phi$. We consider $V(I)$ and $P(I)$ as fundamental RF discharge data which contain information about a variety of RF discharge parameters. The discharge parameters that follow were derived from the measured $V(I)$ and $P(I)$ characteristics. For ease of use we have listed the data as I, V, and P in digital form in Table I. The common features of $V(I)$ are a nearly linear dependence between voltage and current at higher discharge current and a trend toward saturation in discharge voltage at lower current (the last feature is pronounced at higher gas pressures). Linear $V(I)$ characteristics have been found previously for RF discharges in mercury vapor [16], [17] and helium [18] at 40.8 MHz. The overall shape of $V(I)$ is a consequence of both the plasma voltage and RF sheath width being nearly independent of discharge voltage and current [19]–[21].

The RF power characteristics $P(I)$ presented in Figs. 4(a)–(d) and 5(a)–(d) demonstrate a nearly linear dependence on I at small current and high pressure and a nearly I^2 dependence at high discharge current and low gas pressure. This transition from a linear to a squared dependence on current reflects a change in the plasma species into which RF power is dissipated. Thus RF power is dissipated mainly in electrons in the bulk plasma at lower current, and mainly in ions in the RF sheath at higher current [22], [10], [15].

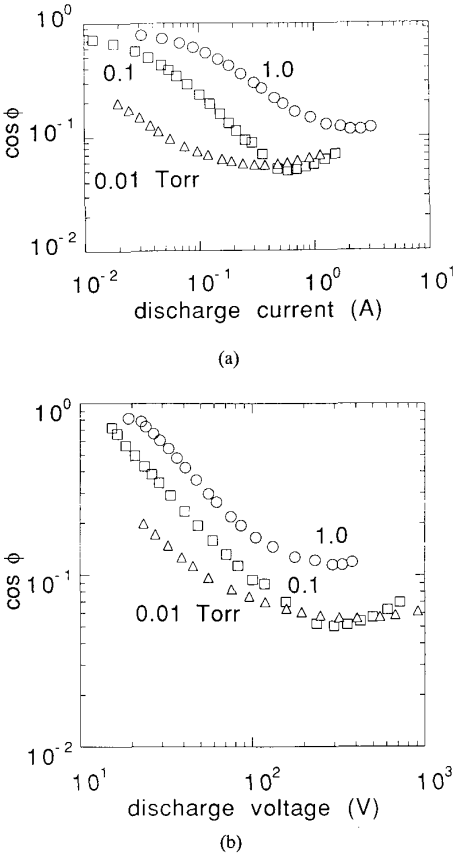

Fig. 3. (a) $\cos\phi$ versus discharge current; and (b) $\cos\phi$ versus discharge voltage.

The transition from one dissipation channel to another occurs at higher discharge current as the gas pressure increases. The subject of electron and ion power distribution will be addressed in more detail in Section III-E.

C. Impedance Characteristics

An alternative way to characterize RF discharge characteristics is through its impedance components. Here, we have chosen to represent the discharge as an equivalent series discharge resistance $R = V\cos\phi/I$ and an equivalent series discharge capacitance $C = I/\omega V\sin\phi$. This representation is elementary yet meaningful, since discharge capacitance straightforwardly relates to RF sheath width, and discharge resistance relates to electron heating in the plasma body and ion acceleration loss in the sheaths. The current dependence of equivalent discharge resistance R and capacitance C is given in Figs. 6(a)–(d) and 7(a)–(d). Over a wide range of gas pressure with increasing current there is generally a substantial current range where $R \propto I^{-1}$ (at smaller currents). With increasing current $R(I)$ reaches a minimum and afterwards slowly increases. Such behavior of the discharge resistance with discharge current has been considered [10] to be a transition from plasma-dominated resistance at low current

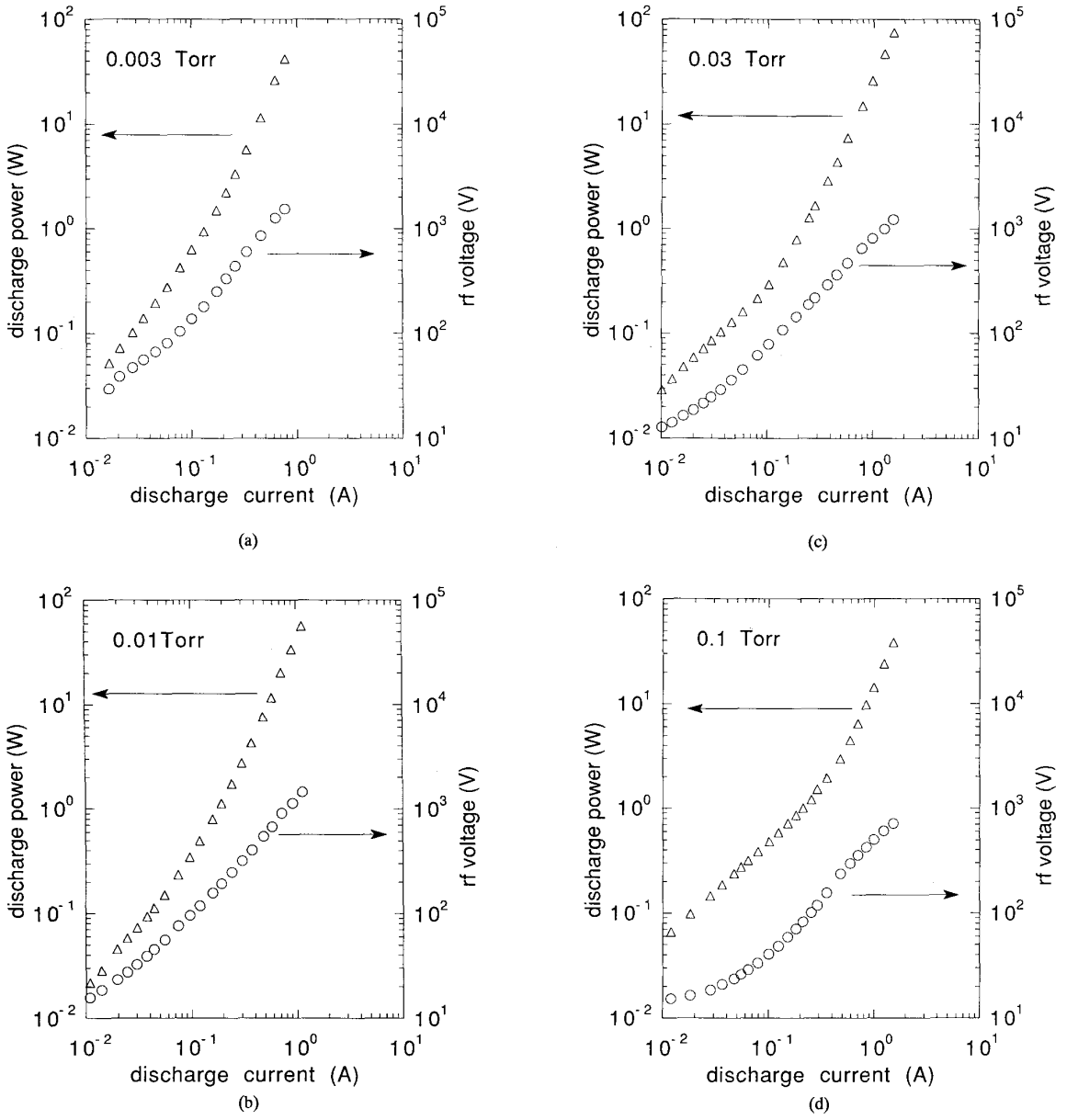

Fig. 4. Discharge voltage and power versus discharge current. (a) $p = 0.003$ torr. (b) $p = 0.01$ torr. (c) $p = 0.03$ torr. (d) $p = 0.1$ torr.

when $R \propto I^{-1}$ to sheath-dominated resistance due to ion acceleration by the dc sheath voltage across the sheath. C is generally constant for all currents at low gas pressure (below 0.1 torr). At larger gas pressure, the capacitance initially grows nearly linearly with discharge current and reaches a fairly constant value at higher levels of current as the gas pressure increases. At 3 torr, neither a minimum in R nor a plateau in C is reached.

The pressure dependence of discharge voltage, power, resistance, and capacitance for two fixed discharge current densities 1 and 10 mA/cm^2 are given in Fig. 8(a) and (b). In both, one can see that $P \propto R$ and $V \propto C^{-1}$, the latter relation implying that the applied discharge voltage mainly drops across the capacitive RF sheaths. More detailed discussion of the data will be given after analysis of the RF discharge equivalent circuit.

D. RF Discharge Equivalent Circuit

It has been pointed out by many authors that measuring the electrical characteristic of an RF discharge can provide information about the discharge parameters such as the sheath width, ion current to the electrodes, and plasma density, and this sometimes makes it possible to delineate between the RF power going into electron heating in the bounded plasma and

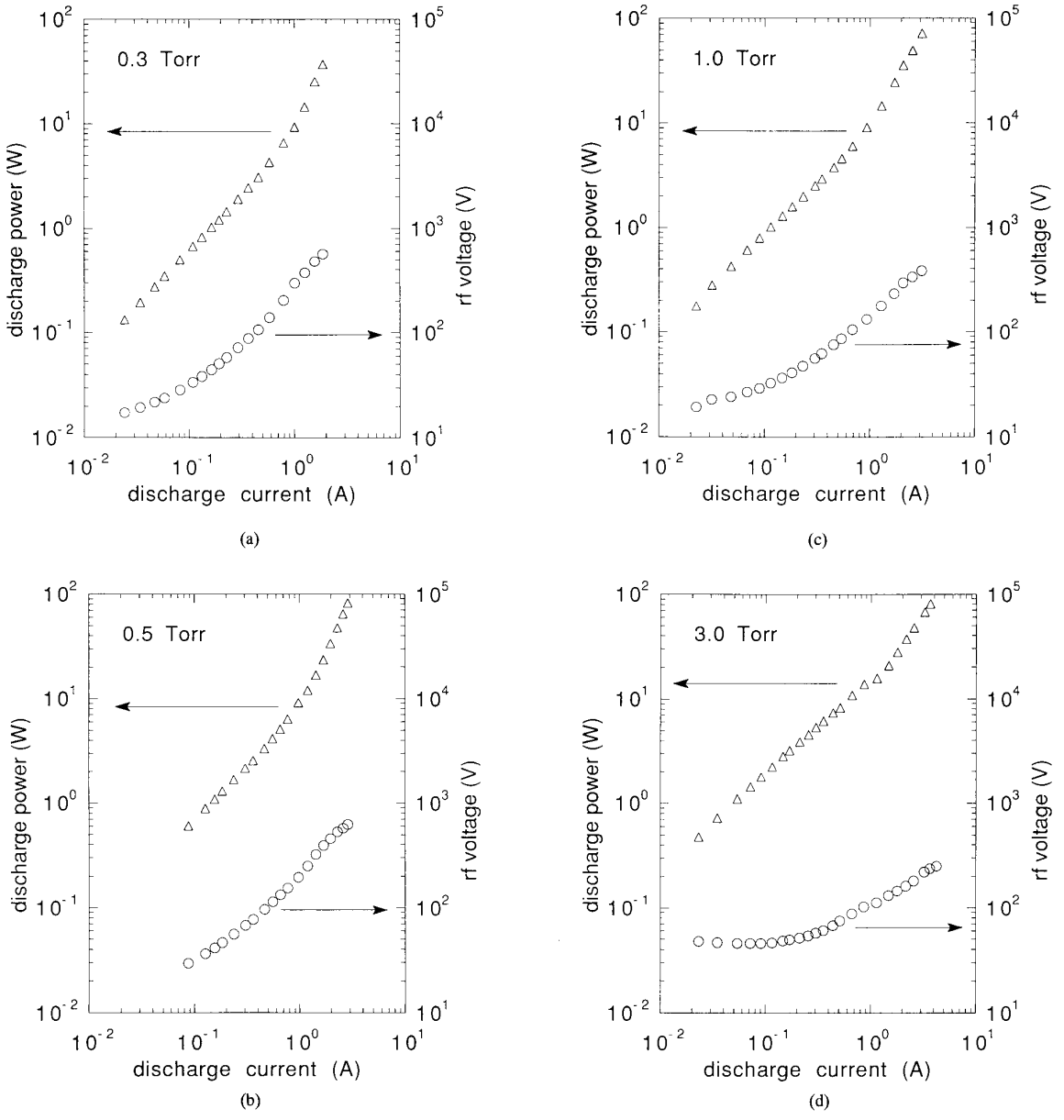

Fig. 5. Discharge voltage and power versus discharge current. (a) $p = 0.3$ torr. (b) $p = 0.5$ torr. (c) $p = 1.0$ torr. (d) $p = 3.0$ torr.

the power going into ion acceleration in the electrode sheaths. To our knowledge, however, attempts to infer discharge and plasma parameters from the measured electrical RF discharge characteristics (mainly impedance) have been based on a number of simplifying assumptions, some of which have a limited applicability to real experiments.

Among these simplifications, the assumption of a purely resistive homogeneous plasma with collision-controlled resistivity is very common. This concept of a bounded RF discharge plasma does not account for stochastic RF power dissipation which is dominant in low-pressure RF discharges. Also, this approach neglects an essential difference (especially at high pressure) between the plasma density n_1 at the plasma–sheath interface and that n_0 at the plasma center (midplane). Often in the literature the relation $n_1 = 0.6n_0$ is used. Having been borrowed from plasma probe theory, this relation is simply inapplicable to the bounded RF discharge plasma [23].

At some conditions the plasma body reactance due to electron inertia and/or displacement current can seriously affect the plasma impedance and should be taken into account for an adequate description of discharge impedance. An example of the influence of electron inertia on the plasma body

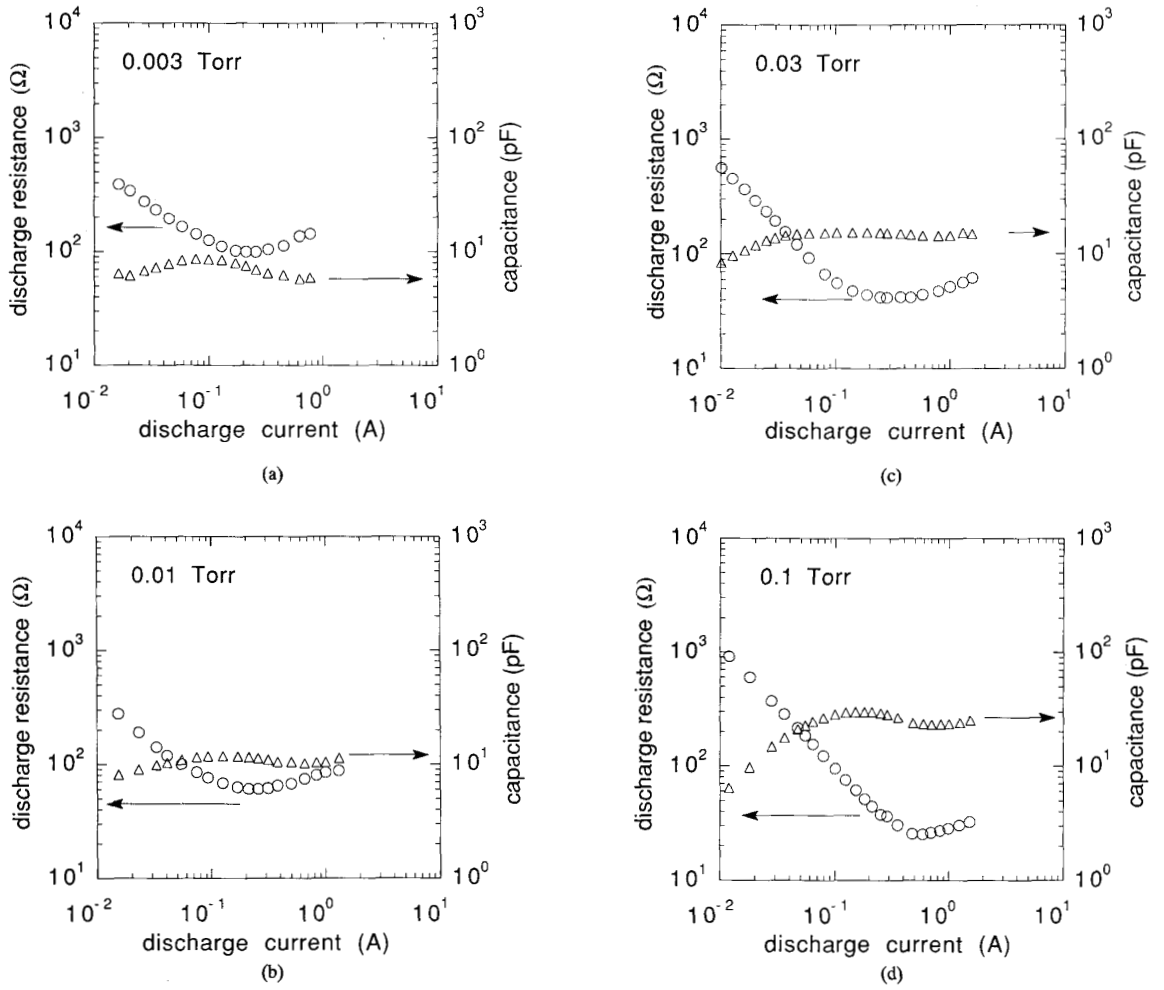

Fig. 6. Equivalent discharge resistance and capacitance versus discharge current. (a) $p = 0.003$ torr. (b) $p = 0.01$ torr. (c) $p = 0.03$ torr. (d) $p = 0.1$ torr.

impedance is resonant RF discharges where sheath and plasma reactances are mutually compensated [24], [25]. The cases where displacement current influences the plasma impedance occur in this experiment for 3 and 1 torr at low discharge current and are discussed later.

Another generally used assumption is the proportionality between dc (V_{dc}) and RF (V_{sh}) components of the sheath voltage, and the assumption that V_{sh} is equal to the discharge voltage V. As we will show in subsection F, these assumptions are fulfilled only for the highest discharge voltages (more than a few hundred volts).

To analyze the relationship between measured electrical characteristics with various RF discharge parameters and find a region of validity for possible simplification, we consider an RF discharge circuit model (Fig. 9(a)) first proposed by Schneider [26] and modified here to take into account ion acceleration losses [4], [18] and stochastic electron heating [27], [19] by introducing additional resistances R'_{sh} and R_{st}. In accordance with the sandwich-like structure for the RF discharge (sheath–plasma–sheath), the equivalent circuit consists of two subcircuits in series representing the plasma body (R_{st}, R_ν, L_0, and C_0) and both electrode sheaths (C'_{sh} and R'_{sh}). The plasma body components R_ν and L_0 represent the plasma resistance due to electron collisions with gas atoms, and the plasma inductance due to electron inertia in the RF field. Corresponding to the plasma conductivity formula $\sigma = e^2 n/m(n + j\omega)$, R_ν and L_0 may be written as:

$$R_\nu = 2d\nu m/Ae^2 n \text{ and } L_0 = 2dm/Ae^2 n. \quad (1)$$

Here, ν is the electron–atom collision frequency, ω is the angular RF driving frequency, m and e are the electron mass and charge, d is the plasma body half-width, A is the discharge cross section, and n is the averaged bulk plasma density. Additional plasma resistance R_{st} corresponding to stochastic electron heating on the oscillating plasma boundaries can be evaluated as follows [19], [17]:

$$R_{st} \approx 2\vartheta_{te} m/Ae^2 n_1 \quad (2)$$

where ϑ_{te} is the electron thermal velocity.

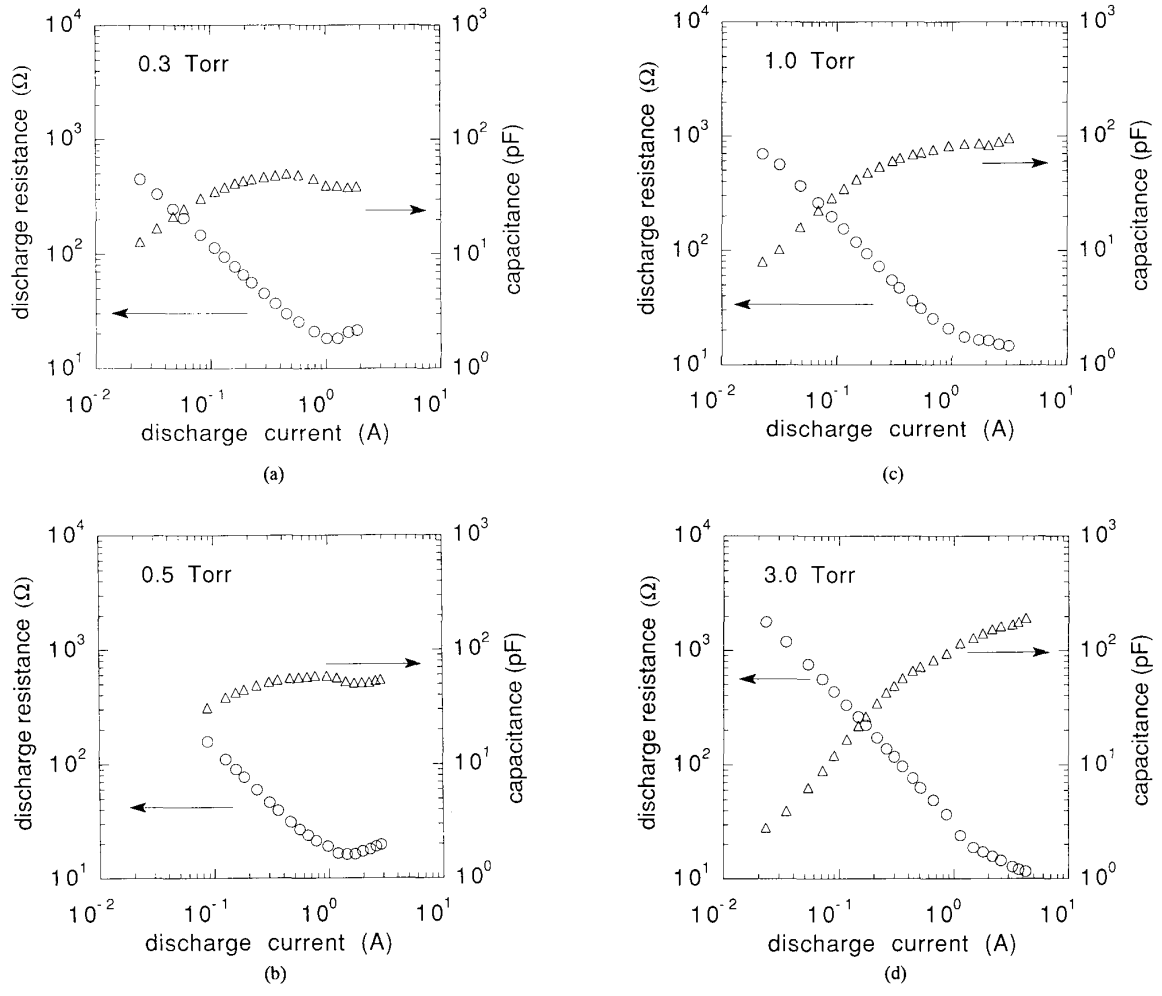

Fig. 7. Equivalent discharge resistance and capacitance versus discharge current. (a) $p = 0.3$ torr. (b) $p = 0.5$ torr. (c) $p = 1.0$ torr. (d) $p = 3.0$ torr.

The capacitor C_0 represents the displacement current through the volume occupied by the plasma body and is:

$$C_0 = A\varepsilon_0/2d \tag{3}$$

where ε_0 is the vacuum dielectric constant. Note that C_0 is not equal to the electrode gap capacitance, since $L = 2(d + S_0)$. The RF electrode sheaths are presented in circuit "a" of Fig. 9 by the parallel sheath capacitance $C'_{\rm sh}$ and by the parallel sheath resistance $R'_{\rm sh}$ (each accounting for both electrode sheaths). The sheath capacitance $C'_{\rm sh}$ determines the effective (capacitive) sheath width S_0 as follows:

$$C'_{\rm sh} = A\varepsilon_0/2S_0. \tag{4}$$

The parallel sheath resistance $R'_{\rm sh}$ represents ion acceleration power in the sheaths P_i in terms of the RF voltage drop across the sheaths $V_{\rm sh}$ as follows [4]:

$$R'_{\rm sh} = V^2_{\rm sh}/2P_i = V^2_{\rm sh}/4I_iV_{\rm dc}. \tag{5}$$

Here, I_i is the ion current to the RF electrode, and $V_{\rm dc}$ is the dc voltage across each (individual) sheath. Another way to account for ion power loss is through an equivalent series resistance in terms of discharge current [10], [21], [15]:

$$R_{\rm sh} = 2P_i/I^2 = 4I_iV_{\rm dc}/I^2. \tag{6}$$

Computing the plasma impedance from circuit "a" in Fig. 9 and (1)–(5) we obtain:

$$Z_p = R_p + jX_p$$

where

$$R_p = (R_{\rm st}+R_\nu)[\omega^2\nu^2_{ef}/\omega^4_e+(1-\omega^2/\omega^2_e)^2]^{-1} \equiv (R_{st}+R_\nu)Q_1 \tag{7}$$

and

$$X_p = (\omega C_0)^{-1}(\omega^2_e - \nu^2_{ef} - \omega^2)[\nu^2_{ef} + (\omega - \omega^2_e/\omega)^2]^{-1} \equiv (\omega C_0)^{-1}Q_2 \tag{8}$$

with $\nu_{\rm ef} = \nu(1 + R_{\rm st}/R_\nu)$ and the electron plasma frequency ω_e defined as $\omega^2_e = e^2n/\varepsilon_0 m$. Transforming the parallel sheath

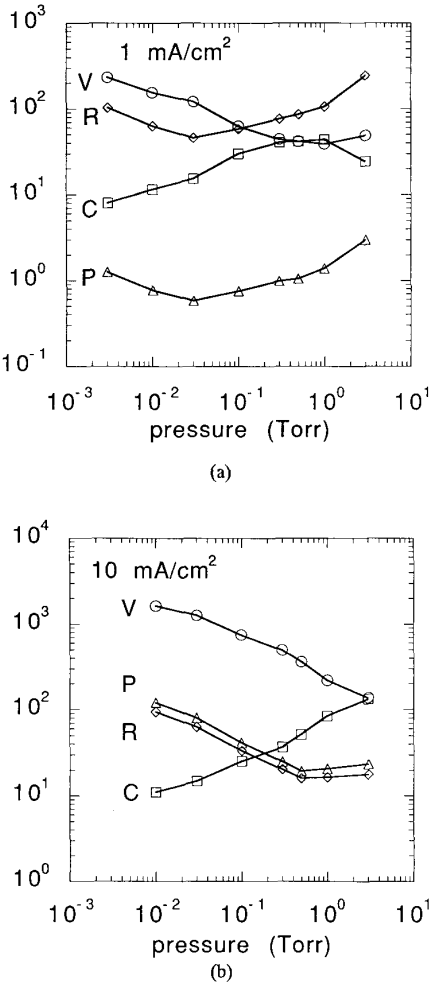

Fig. 8. RF discharge voltage, power, resistance, and capacitance versus gas pressure at two current densities: 1 and 10 mA/cm^2.

circuit to a series circuit, we obtain:

$$R_{\rm sh} = R'_{\rm sh}[1 + (\omega C'_{\rm sh} R'_{\rm sh})^2]^{-1} \equiv 4I_i V_{\rm dc}/I^2 \qquad (9)$$

$$C_{\rm sh} = C'_{\rm sh}[[1 + (\omega C'_{\rm sh} R'_{\rm sh})^2]/(\omega C'_{\rm sh} R'_{\rm sh})^2]. \qquad (10)$$

Evaluation of $(\omega C'_{\rm sh} R'_{\rm sh})^2$ based on experimental data shows that it is always more than 100 and therefore with high accuracy, $C_{\rm sh} = C'_{\rm sh}$. Finally, for the RF discharge resistance and capacitance, we obtain from (5)–(8):

$$R = R_{\rm sh} + Q_1(R_{\rm st} + R_\nu) \qquad (11)$$

$$C = C_{\rm sh}(1 - Q_2 C_{\rm sh}/C_0)^{-1}. \qquad (12)$$

Even for a homogeneous plasma, the coefficients Q_1 and Q_2 in (11) and (12) are rather complicated functions (see (7) and (8)) of plasma parameters and driving frequency. An example of the plasma impedance with an inhomogeneous plasma density distribution can be found in [28], where the corresponding results must be expressed through integral equations. With regard to (11) and (12), it is apparent that the plasma density can be inferred from the plasma collisional resistivity using (1) only if $R_\nu \gg R_{\rm st}$, $R_{\rm sh}$, and $Q_1 = 1$. Similarly, the sheath width can be inferred from the RF discharge capacitance using (4) only when $|Q_2| \ll C_0/C_{\rm sh} = S_0/d$. Note that Q_2 may be either positive or negative. For example, in a resonant RF discharge $Q_2 = S_0/d$, but in our experiments Q_2 is negative.

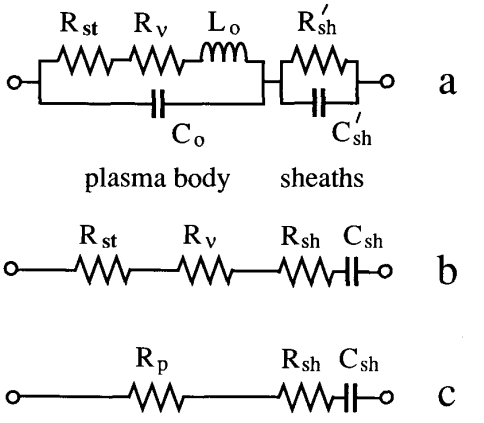

Fig. 9. (a) Equivalent circuits representing an RF discharge for various levels of simplification. (b) is equivalent to (a) when$Q_1 = 1$ and $Q_2 \ll S_0$ / d. (c) is equivalent to (b) with $R_p = R_s + R_\nu$.

Probe measurements which will be published elsewhere were performed under discharge conditions of the present work and showed that for all cases $\omega_e^2 \gg w^2$ and $\nu_{\rm ef}^2 \gg \omega^2$; thus the coefficients Q_1 and Q_2 may be written in a more compact form:

$$Q_1 = [1 + \omega^2 \nu_{ef}^2/\omega_e^4]^{-1}$$

and

$$Q_2 = [\omega_e^2/\nu_{\rm ef}^2 - 1] \cdot [1 + \omega_e^4/\omega^2 \nu_{\rm ef}^2]^{-1}. \qquad (13)$$

The factor $Q_2 \cdot d/S_0$ characterizes the bulk plasma reactivity which influences the inferred values of sheath capacitance $C_{\rm sh}$ and sheath width S_0. Estimations show that $Q_2 \cdot d/S_0$ is larger or comparable to unity along the axis for the peripheral plasma outside the midplane of the discharge at 3 torr with discharge currents less than about 0.3 A, and at 1 torr with the smallest discharge currents. For these conditions the RF field penetrates the peripheral plasma, since its relative permittivity is near unity and results in an increase in the discharge capacitive impedance, such that for the smallest discharge current, the discharge capacitance approaches the electrode gap capacitance $C_0 = A\epsilon_0/L = 2.1$ pF (see Fig. 7(c) and (d)). Thus calculation of the sheath width for the smallest discharge current at 3 torr from discharge capacitance (assuming $Q_2 = 0$) results in an order larger value of S_0 than is actually (visibly) observed.

The axial plasma distribution depends on Q_2 for high gas pressure where the ionization frequency is a local function of

the plasma RF field. For $Q_2 \approx -1$ there is a homogeneous RF field in the transparent (not opaque) plasma, and the ionization frequency does not depend on its axial coordinate. In this case, the axial plasma density distribution $n(x)$ coincides with a Schottky distribution: $n(x) \propto \cos(\pi x/2d)$. For $|Q_2| \ll S_0/d$, the RF field $E_p(x)$ and plasma density profile are coupled due to the continuity of the discharge current, such that $E_p(x) \propto [n(x)]^{-1}$. Under this condition, the plasma density profile becomes flat with a sharp fall off at its boundaries, while the RF field and ionization rate peak near the plasma boundaries [29], [30]. This electron heating and ionization enhancement on the plasma boundaries was known long ago [29], but today is often misleadingly referred to in the literature as "collisional wave riding"; likewise, stochastic electron heating on the plasma boundaries has been labeled "wave riding." In both cases the term "wave riding" (associated in plasma physics with Landau damping) is irrelevant in application to RF discharges where the driving frequency is generally far below the plasma frequency.

In further analysis we will assume that$|Q_2| \ll S_0/d$. This condition excludes inferring sheath width in the high-pressure, low-current regime where the results are sensitive to Q_2. With $|Q_2| \ll S_0/d$, the equivalent circuit "a" in Fig. 9 reduces to circuit "b," where the parameters relate to the measured discharge impedance components R and C as follows:

$$R_\nu + R_{\rm st} + R_{\rm sh} = R, \text{ and } C_{\rm sh} = C. \tag{14}$$

It is convenient to represent the discharge resistance as a sum of two components (Fig. 9(c)):

$$R = R_p + R_{\rm sh} \tag{15}$$

where $R_p = R_{\rm st} + R_\nu$. The first term in (15) is the plasma resistance corresponding to RF power dissipated in electron heating (collisional and stochastic); the second term is sheath resistance corresponding to RF power dissipated in the sheaths for ion acceleration by the rectified (dc) sheath voltage.

In accordance with equivalent circuit "c" in Fig. 9, the RF voltage across the two sheaths is:

$$V_{\rm sh} = [V^2 - V_p^2 - 2V_pV_s]^{1/2}. \tag{16}$$

Here, $V_p = IR_p$ is the RF voltage across the plasma (including the voltage drop on its boundary due to stochastic electron heating), and $V_s = IR_{\rm sh}$ is the ohmic part of the RF sheath voltage corresponding to the ion power loss. The sum of V_p and V_s constitutes the ohmic component of the discharge voltage; i.e.,

$$V_p + V_s = V\cos\phi. \tag{17}$$

Further analysis of the experimental data will be based on the equivalent circuit "c" in Fig 9.

E. Plasma Voltage and Sheath Resistance

Both of these parameters are fundamental for RF discharges, since they quantify the different power dissipation channels in the discharge. From the equivalent series circuit "c" in Fig. 9, the total RF power consumed by the discharge can be written:

$$P = 1/2 \cdot IV_p + 1/2 \cdot I^2R_{\rm sh}. \tag{18}$$

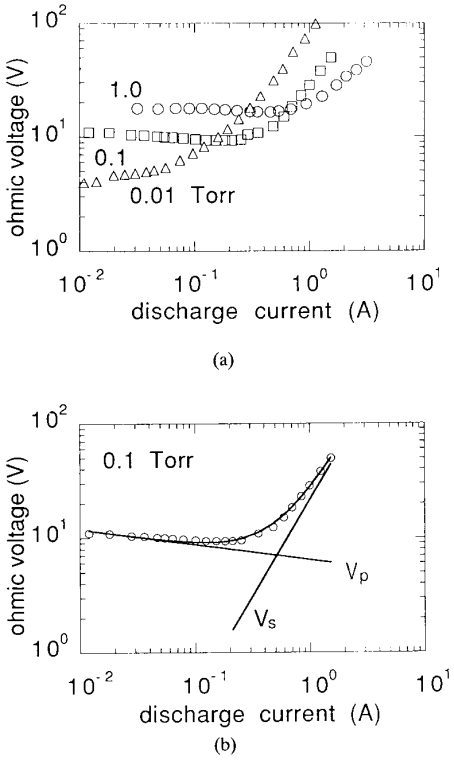

Fig. 10. Ohmic voltage versus discharge current (a) for three gas pressures 0.01, 0.1, and 1.0 torr, and (b) an example ofV_s and V_p found through curve-fitting.

Due to the ionization balance in weakly ionized gas discharge plasmas (irrespective of dc or RF driven), the voltage across the bulk plasma is nearly independent of the discharge current. Thus the bulk plasma component of total discharge power is nearly proportional to the discharge current and for small currents (as given in (18)) is equal to the total discharge power. Consequently, in this current range the discharge resistance is inversely related to the discharge current, and the ohmic part of the discharge voltage $V\cos\phi$ is nearly constant. From (18), one should expect: $P \propto I^2$, a saturation in discharge resistance for large I, and a linear growth in the ohmic part of the discharge voltage $V\cos\phi$. Indeed, such current dependent behavior is readily apparent in the data presented in Figs. 4–7 and 10. The change in the functionality of $P(I)$, $R(I)$, and $V\cos\phi(I)$ with increasing discharge current corresponds to a transition in RF power transfer channels from electron heating to ion acceleration. This change in functionality of $P(I)$, $R(I)$, and $V\cos\phi(I)$ can be used to infer separately electron power $P_e = 1/2 \cdot IVp$ and ion power $P_i = 1/2 \cdot I^2R_{\rm sh}$ or, equivalently, to find V_p and $R_{\rm sh}$. Such a procedure has been done with the experimental data of $R(I)$[10] and $P(I)$[15]. An example of the separation between the electron and ion power found in [15] is given in Fig. 11. Here we demonstrate a similar procedure using the current dependence of $V\cos\phi(I)$ given in Fig. 10. This approach appears to be a convenient and relatively accurate way to infer separately V_p and $R_{\rm sh}$,

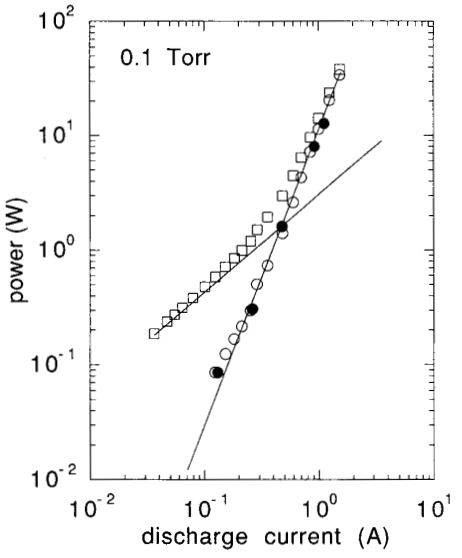

Fig. 11. Inferred ion acceleration power (○) determined from measured total discharge power (□). Ion power found from ion current measurements [15] (•) are shown for comparison.

since $V\cos\phi \approx V_p$ at small discharge current and large gas pressure (thus giving a direct indication of the plasma voltage and its dependence on current and gas pressure), while $d(V\cos\phi)/dI \approx R_{sh}$ at large current and low gas pressure.

The values of V_p and R_{sh} were found as functions of the discharge current for each gas pressure by fitting the experimental values of $V\cos\phi$ to formula (17) with the approximations $V_p = BI^b$ and $R_{sh} = CI^c$, i.e., $V\cos\phi = V_p + IR_{sh} = BI^b + CI^{c+1}$, where B, b, C, and c are constants found by numerical curve fitting. An example of this procedure is shown in Fig. 10(b), where two components of $V\cos\phi$ look, in logarithmic scale, like straight lines. Note that the accuracy of the inferred functions V_p and R_{sh} depends on the range of the discharge current where experimental data for $V\cos\phi$ are available. This accuracy can be different for V_p and R_{sh}. For low gas pressure and/or high discharge current when the discharge power goes mainly for ion acceleration, the sheath resistance R_{sh} is inferred with high accuracy at the expense of the poor accuracy in V_p. Alternately, for high gas pressure and/or low discharge current when discharge power goes mainly into electron heating, we attain accurate values of V_p and less certainty in R_{sh}. Therefore the data for V_p at the lowest gas pressure (3 mtorr), and the data for R_{sh} for the highest pressure (3 torr) are the least reliable.

The plasma voltage $V_p = BI^b$ found with this technique is given in Fig. 12. For all gas pressure we observed a slightly falling $V_p(I)$ characteristic similar to the well-known voltage drop across the positive column of a dc discharge. As in dc discharges, the negative static V/I characteristic for RF plasma is due to changes in plasma neutrality (transition from free to ambipolar diffusion), in the electron energy distribution function, and in the ionization mechanism from direct to multistep ionization. What is remarkable is that the falling $V_p(I)$ characteristic occurs in RF discharges with either collisional or

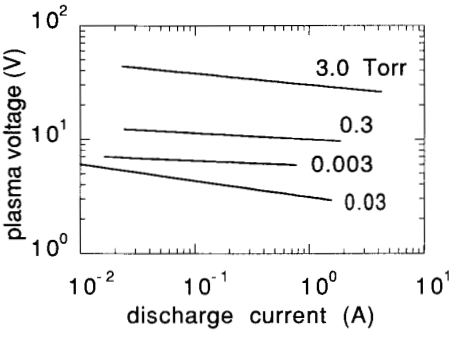

Fig. 12. Plasma voltage versus discharge current for four gas pressures: 0.003, 0.03, 0.3, and 3.0 torr.

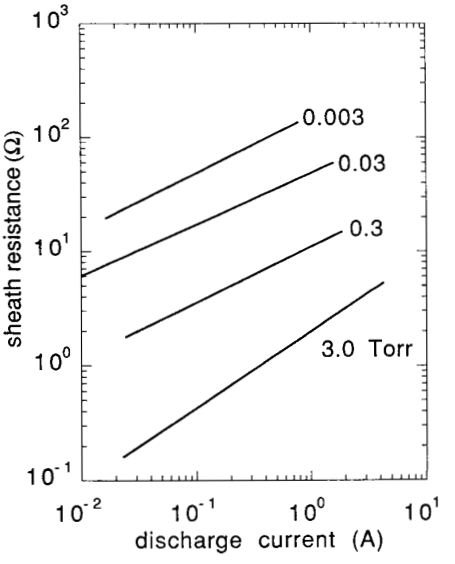

Fig. 13. Sheath resistance versus discharge current for four gas pressures: 0.003, 0.03, 0.3, and 3.0 torr.

stochastic-dominated heating. Probe measurements carried out for this discharge [31] showed an abrupt transition between the collisional and stochastic heating mode at $p \approx 0.05$ torr, similar to that found in argon RF discharges [13] with $L = 2$ cm.

The sheath resistance values found as $R_{sh} = CI^c$ are given in Fig. 13 as a function of discharge current. For all gas pressure (except $p = 0.1$ torr), R_{sh} is nearly proportional to $I^{1/2}$. This agrees with experimental data and calculation [10] for a collisional dc model of an RF sheath. One can also show that similar calculations for a collisionless sheath based on Child–Langmuir law or a more relevant dynamic model [32] yield $R_{sh} \propto V_{sh}^{1/2}$. Since the discharge capacitance is nearly independent from the discharge current (except for small discharge current and large gas pressure), $V_{sh} \propto I$ and therefore $R_{sh} \propto I^{1/2}$ should be expected for all the range of gas pressure. The "irregular" dependence of $R_{sh}(I)$ at $p = 0.1$ torr, where we found $R_{sh} \propto I^{2/3}$, probably is related to the transition between collisional and stochastic heating mode

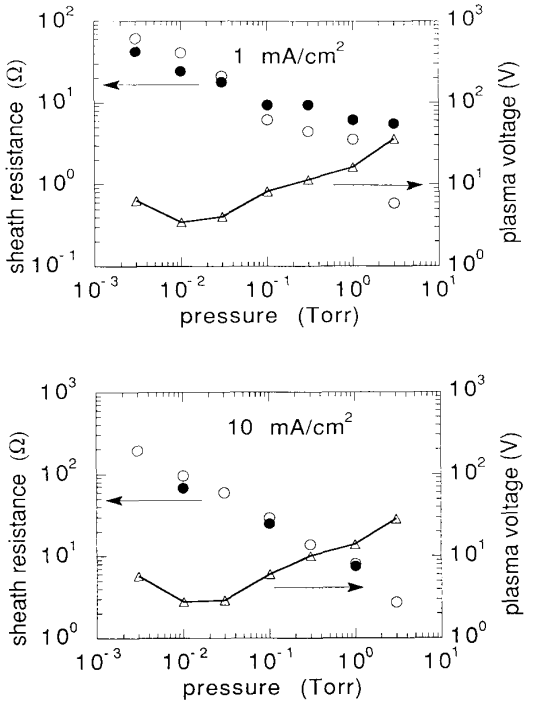

Fig. 14. Sheath resistance (○ and •) and plasma voltage (△) versus gas pressure for 1 mA/cm^2 and 10 mA/cm^2. (○) are based on our measured data, and (•) are based on ion current measurements [15].

occurring near this pressure, where the plasma parameters are found to be very sensitive to changes in discharge current.

The gas pressure dependence of the plasma voltage $V_p(p)$ and sheath resistance $R_{\rm sh}(p)$ are given in Fig. 14 for discharge current densities of 1 and 10 mA/cm^2. For comparison, $R_{\rm sh}$ obtained independently from ion current and dc sheath voltage measurements is shown for the same discharge conditions [15]. As one can readily see, there is reasonable agreement in $R_{\rm sh}$ obtained by the two different methods except in the case of $p = 3$ torr, where derivation of $R_{\rm sh}$ becomes uncertain. For large discharge current (10 mA/cm^2) where P_i is a considerable part of the total discharge power and therefore can be found with relatively high accuracy, there is remarkable agreement between data obtained by two independent methods. The pressure dependence of the sheath resistance is close to $R_{\rm sh} \propto p^{-1/2}$ for all range of gas pressure; this result follows from calculation based on a dc model of a collisional RF sheath [10]. Note that even for the lowest gas pressure ($p = 3$mtorr), the ion mean free path $\lambda_i = 1.4$ cm is close to the RF sheath width $S_0 \approx 1$ cm.

The pressure dependence of the plasma voltage is close to $V_p \propto p^{1/2}$ for the collisionally dominated regime. At this condition the plasma RF electric field can be readily estimated as $E_p \approx V_p/2d$ since $\nu^2 \gg \omega^2$, and at this rather high pressure $E_p(x) \propto n(x)^{-1}$ and the plasma axial distribution is for the most part homogeneous [30]. At low gas pressure the values of V_p reach a minimum and start to rise at lower gas pressure. Such behavior is absolutely similar to the dependence of $V_p(p)$ obtained in a mercury resonant RF discharge at 40.8 MHz in the pressure range between 0.2 and 20 mtorr, and is related to the purely stochastic electron heating at these low gas pressures [25]. This gives a possibility to evaluate the rate of stochastic heating process on the oscillating plasma boundary from experimental data of V_p, since the RF power dissipation in the plasma body is negligibly small for the stochastic heating mode [33], [34].

The ratio of ion to electron power P_i/P_p can be readily found from the inferred data as follows: $P_i/P_p = IR_{\rm sh}/V_p$. For the conditions of the present work, this ratio varies widely from about 10^{-2} (at lowest current and highest gas pressure) to about 20 (for highest current and lowest gas pressure). Corresponding data are given in [15].

Note that the inferred analytical extrapolations for $V_p(I)$ and $R_{\rm sh}(I)$ may not be valid at high discharge current and voltage due to a discharge transition into the γ-regime [35]. If this occurs, V_p should drop because of a growth in the plasma density (conductivity) caused by secondary electron ionization. At high p/ω there is a "sharp" [35] transition into the γ-regime due to a secondary electron avalanche in the RF sheaths (γ-process). This may change the functionality of $R_{\rm sh}(I)$, since both the ion current and sheath width could be affected by the γ-process. Probe measurements conducted for the experimental conditions of the present work showed that for $p \geq 0.1$ torr and the highest discharge voltages, there was a "smooth" discharge transition into the γ-regime accompanied by a step-like drop in the electron mean energy, along with a steep rise in the plasma density, but with no appreciable change in the discharge electrical characteristics. Only at $p = 3$ torr (where V_p is comparable to total discharge voltage) does the drop in V_p within the γ-regime appear to result in some irregularities in $P(I)$, $V(I)$, and $C(I)$ when $I \approx 1$A (see Figs. 5(d) and 7(d)).

F. Sheath Voltage

Having found the plasma voltage and sheath resistance, one can evaluate the RF sheath voltage $V_{\rm sh}$ across the RF sheaths on both plasma boundaries. Using (16) and noting that $V_s = IR_{\rm sh}$ we obtain:

$$V_{\rm sh} = [V^2 - V_p^2 - 2V_pIR_{\rm sh}]^{1/2}. \tag{19}$$

The calculated values of $V_{\rm sh}$ are presented in Figs. 15–17 as functions of the discharge voltage. Here also the dc component of the individual sheath voltage $V_{\rm dc}$ is given. The values of $V_{\rm dc}$ were computed from the dc voltage V_0 measured between the discharge electrodes and a floating Langmuir probe in the midplane of the discharge [14], and from probe measurements of the voltage difference V_f between the floating probe and plasma potential ($V_{\rm dc} = V_0 + V_f$). It is apparent from Figs. 15–17 that only at high discharge voltage and low gas pressure is the RF sheath voltage equal to the applied discharge voltage and the dc sheath voltage proportional to the discharge voltage. For moderate sheath voltage and higher gas pressure, neither $V_{\rm sh} = V$ nor $V_{\rm dc} \propto V_{\rm sh}$ is valid, contrary to prevalent lore. A rapid fall in $V_{\rm sh}$ at low discharge voltage and high gas pressure is the result of the RF voltage redistribution

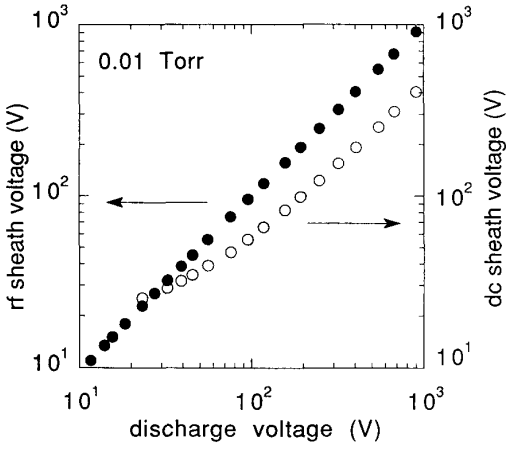

Fig. 15. RF (•) and dc (○) sheath voltage versus RF discharge voltage for $p = 0.01$ torr.

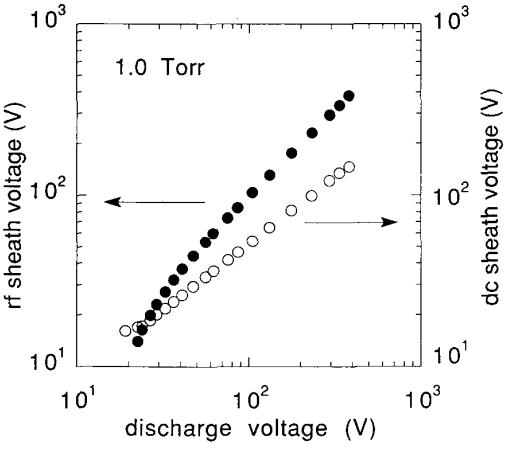

Fig. 17. RF (•) and dc (○) sheath voltage versus RF discharge voltage for $p = 1.0$ torr.

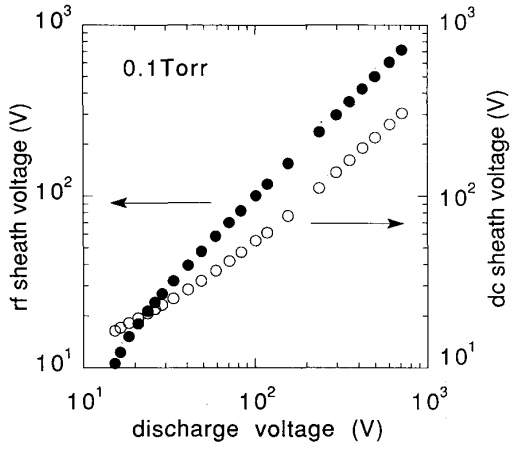

Fig. 16. RF (•) and dc (○) sheath voltage versus RF discharge voltage for $p = 0.1$ torr.

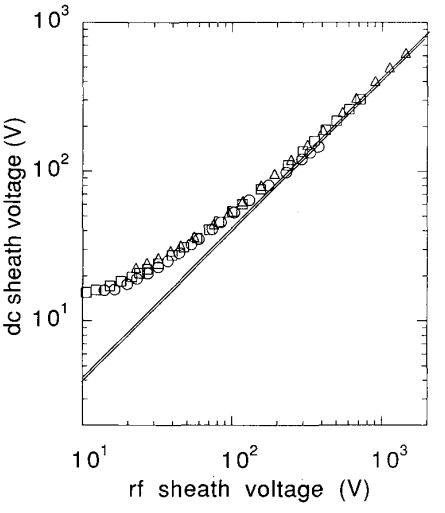

Fig. 18. Dc sheath voltage versus RF sheath voltage for three gas pressures: 0.01; 0.1; and 1.0 torr. The solid lines are dc sheath voltages from collisionless [32] (upper line) and collisional [39] (lower line) dynamic sheath models.

between RF sheaths and the plasma body, while opposite trends in the V_{dc} behavior are the result of residual sheath effect. This last point is demonstrated in Fig. 18, where V_{dc} is shown as a function of the RF sheath voltage for different gas pressure. As the RF sheath voltage decreases, the dc sheath voltage approaches a limit (the dc floating voltage V_f) which corresponds to a few electron mean energies. This reflects a trivial fact that a positively charged electrode sheath exists even without RF sheath voltage. As has been shown [36], [21], accounting for the residual sheath in the sheath capacitance calculation allows one to explain the linearity in the RF discharge current/voltage characteristics.

G. Sheath Width

The sheath width S_0 was calculated assuming the plasma reactance to be negligible. This limits the range of validity to a regime where the discharge current is sufficiently high and the gas pressure is not too large, as was mentioned in subsection D. Note that S_0 is considered as a capacitive sheath width relating to the ratio of RF sheath voltage to current. The values of S_0 calculated as $S_0 = A\varepsilon_o/2C$ are given in Fig. 19 as a function of the RF sheath voltage for different gas pressure. Visual sheath widths found "by eye" and corresponding to the distance between the electrode and plane of maximum contrast are given for comparison. Generally, the visual sheath widths were 1.5–2 times larger than the capacitive sheath widths. This difference was noticed in helium [18] RF discharges and is the result of the fact that the maximum in the visual contrast takes place at the position where the oscillating sheath is farthest away from the electrode, while the capacitive sheath width is related to some averaged sheath position which should always be smaller than the maximum sheath width. As seen in Fig. 19, the sheath width rapidly grows when the RF sheath voltage

TABLE I
TABLES OF DISCHARGE CURRENT (I), VOLTAGE (V), AND POWER (P) FOR EIGHT DIFFERENT GAS PRESSURES BETWEEN 0.003 AND 3.0 TORR

0.003 torr

current (A)	voltage (V)	power (W)
0.0164	29.4	0.0516
0.0206	38.7	0.0721
0.0274	47.0	0.102
0.0348	55.7	0.139
0.0450	66.8	0.195
0.0583	80.9	0.277
0.0775	105	0.424
0.100	138	0.628
0.130	180	0.936
0.172	252	1.49
0.212	334	2.22
0.259	436	3.32
0.331	600	5.71
0.453	851	11.5
0.622	1.26*e*+03	26.3
0.772	1.54*e*+03	42.1

0.01 torr

current (A)	voltage (V)	power (W)
0.00259	7.77	0.00425
0.00388	9.04	0.00701
0.00531	10.4	0.0100
0.00673	11.6	0.0129
0.00919	14.0	0.0181
0.0109	15.6	0.0216
0.0140	18.4	0.0283
0.0197	23.2	0.0456
0.0245	27.3	0.0577
0.0303	32.4	0.0728
0.0376	39.0	0.0932
0.0441	45.3	0.113
0.0557	55.7	0.150
0.0744	75.8	0.233
0.0962	95.6	0.345
0.120	118	0.495
0.159	157	0.794
0.192	192	1.13
0.241	247	1.73
0.303	319	2.74
0.373	404	4.27
0.484	548	7.60
0.585	673	11.6
0.718	906	20.2
0.914	1.13*e*+03	33.6
1.13	1.44*e*+03	56.2

0.03 torr

current (A)	voltage (V)	power (W)
0.00413	9.45	0.00916
0.00557	10.2	0.0134
0.00792	11.5	0.0219
0.0102	12.7	0.0288
0.0127	14.1	0.0364
0.0162	16.4	0.0477
0.0201	18.6	0.0587
0.0249	21.5	0.0719
0.0297	24.6	0.0853
0.0365	29.0	0.104
0.0461	35.6	0.128
0.0588	45.0	0.160
0.0806	61.7	0.216
0.103	78.6	0.294
0.141	107	0.477
0.189	144	0.786
0.247	188	1.28
0.283	218	1.67
0.371	291	2.88
0.455	361	4.34
0.577	467	7.38
0.789	641	14.8
0.996	803	25.7
1.29	990	46.7
1.56	1.22*e*+03	74.6

0.1 torr

current (A)	voltage (V)	power (W)
0.0120	15.3	0.0662
0.0181	16.4	0.0984
0.0280	18.4	0.146
0.0362	20.8	0.187
0.0470	23.6	0.238
0.0546	26.0	0.274
0.0639	28.7	0.315
0.0792	33.4	0.384
0.101	40.6	0.482
0.124	48.4	0.585
0.153	59.0	0.716
0.182	70.7	0.854
0.212	82.7	0.996
0.253	101	1.20
0.288	118	1.52
0.356	156	1.94
0.481	236	2.96
0.594	297	4.46
0.701	355	6.43
0.843	423	9.67
0.998	499	14.2
1.25	605	23.8
1.54	713	38.2

decreases to small values. One reason for this has been already mentioned and is due to the RF field penetration into the low density highly collisional plasma. Another is related to residual electrode sheath's effect at relatively low RF sheath voltage when the sheath width is controlled mainly by Debye length λ_d and does not depend on the RF sheath voltage [21]. This situation takes place at very small discharge current (less than tens of milliamperes) and is usually accompanied by a fast growth in electron temperature. The combined effect of falling plasma density and rising electron temperature results in the growth of λ_d and S_0 that finally leads to discharge extinction when the sheaths from both electrodes are close to overlapping.

The pressure dependence of S_0 in Fig. 19 appears to be close to $S_0 \propto p^{-1/2}$ consistent with a recent summary for a

TABLE I (*continued*)

0.3 torr			0.5 torr		
current (A)	voltage (V)	power (W)	current (A)	voltage (V)	power (W)
0.0243	17.3	0.132	0.0877	29.3	0.603
0.0342	19.4	0.195	0.127	36.1	0.887
0.0470	21.8	0.273	0.156	41.0	1.09
0.0583	23.9	0.348	0.184	46.1	1.30
0.0823	28.6	0.497	0.238	55.6	1.68
0.109	33.8	0.671	0.305	67.5	2.15
0.132	38.5	0.825	0.362	76.9	2.56
0.163	44.5	1.03	0.464	96.0	3.35
0.193	50.6	1.21	0.557	114	4.15
0.227	57.8	1.45	0.656	133	5.12
0.291	71.8	1.91	0.775	154	6.37
0.365	87.7	2.45	0.979	195	9.14
0.455	106	3.09	1.20	249	12.0
0.580	139	4.26	1.44	321	16.7
0.789	204	6.53	1.70	390	23.4
1.01	297	9.26	1.98	454	33.7
1.26	373	14.4	2.31	526	47.6
1.56	481	25.2	2.60	571	64.5
1.86	563	36.9	2.88	622	82.0

1.0 torr			3.0 torr		
current (A)	voltage (V)	power (W)	current (A)	voltage (V)	power (W)
0.0226	19.1	0.177	0.0232	47.5	0.479
0.0317	22.6	0.281	0.0348	46.4	0.720
0.0481	24.0	0.422	0.0540	45.7	1.10
0.0684	26.7	0.609	0.0718	45.5	1.43
0.0897	29.1	0.795	0.0908	45.7	1.77
0.115	32..6	1.02	0.116	46.2	2.21
0.148	36.5	1.29	0.147	48.2	2.81
0.184	40.9	1.58	0.171	49.2	3.20
0.234	47.4	1.98	0.212	51.3	3.88
0.303	55.9	2.52	0.257	53.9	4.55
0.352	62.2	2.91	0.303	57.3	5.36
0.455	75.5	3.75	0.356	60.7	6.14
0.540	86.3	4.53	0.438	67.5	7.35
0.687	105	5.96	0.512	75.0	8.26
0.936	132	9.02	0.665	87.4	10.9
1.29	177	14.5	0.865	103	13.8
1.72	232	24.3	1.15	112	15.7
2.09	294	35.4	1.48	132	20.6
2.57	335	49.5	1.80	146	27.7
3.14	382	71.6	2.17	161	37.0
			2.58	181	47.7
			3.25	221	67.2
			3.68	238	81.1
			4.24	252	104

large number of experiments in argon asymmetrically driven RF discharges [37]. It is most remarkable that the values of S_0 remain nearly constant over a wide range of RF sheath voltages, especially at low gas pressure. This contradicts ion space-charge-limited models (both collisionless and collisional) which are widely used in RF discharge modeling. Thus for the collisionless case governed by Child–Langmuir law, $S_0 \propto V_{\rm dc}^{3/4} I_i^{-1/2}$. Also, $S_0 \propto V_{\rm sh} I^{-1}$. Noting that $I_i = Aen_1 \vartheta s$ and $I = Aen_1 \vartheta_\sim$, and with the commonly used assumption that $V_{\rm dc} \propto V_{\rm sh}$, one can obtain $S_0 \propto V_{\rm sh}^{1/2} \vartheta_\sim / \vartheta_s$. Here $\vartheta_\sim$ and ϑ_s are the electron oscillatory velocity and the ion sound speed on the plasma–sheath boundary, respectively. The ratio of $\vartheta_\sim / \vartheta_s$ does not depend on discharge current, since both the electron temperature and electric field change little in weakly ionized plasmas. The dependence $S_0 \propto V_{\rm sh}^{1/2}$ implies that the static current/voltage characteristic of low pressure, high voltage ($V^2 \gg V_p^2$) RF discharges should follow the relation, $I \propto V^{1/2}$. To our knowledge, such a current/voltage characteristic has never been demonstrated experimentally. Moreover, nearly linear I/V characteristics ($S_0 \approx$ const) have been obtained in experiments with mercury and helium RF discharges and have been recently demonstrated in particle-in-cell simulations [38], [34]. A similar evaluation for the collisional space-charge-limited sheath yields $S_0 \propto V_{\rm sh}^k$, with k being between $1/3$ and $1/5$ depending on the choice of initial ion velocity; this implies a growing function $S_0(V_{\rm sh})$, while

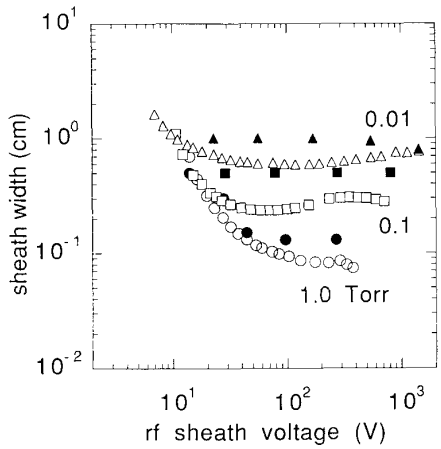

Fig. 19. Sheath width versus RF sheath voltage for three gas pressures: 0.01, 0.1, and 1.0 torr. Open symbols are based on measurements of equivalent sheath capacitance, and closed symbols are visual-observed.

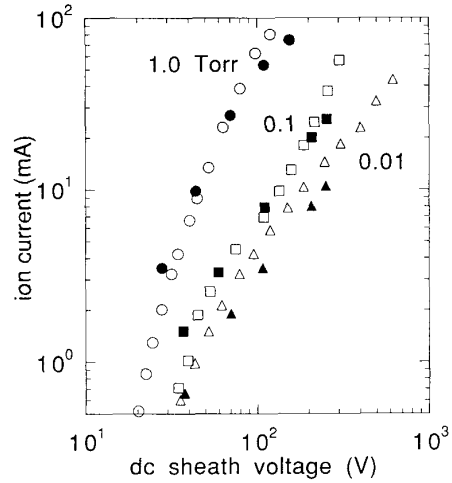

Fig. 20. Ion current versus dc sheath voltage for three gas pressures: 0.01, 0.1, and 1.0 torr. Open symbols are from measured data, and closed symbols are directly measured ion currents [15].

experiments (Fig. 19) corresponding to a highly collisional sheath ($p = 1$ torr) demonstrate an opposite trend.

H. Ion Current

A method generally found in the literature to infer the ion current I_i to an RF electrode is based on Child–Langmuir law or its collisional analog using experimental data of the sheath width (usually obtained photometrically) and dc sheath voltage (usually obtained from measured dc bias voltage). Both measurements may not be of high accuracy for a variety of reasons. Together with these uncertainties and the questionable appropriateness of the Child–Langmuir law for RF sheaths, this evaluation of ion current could contain significant error. An alternative approach we have used to infer ion current is based on measured dc sheath voltage V_{dc} and previously found values of sheath resistance R_{sh} (or ion power P_i) inserted into the following expression: $P_i = 2V_{dc}I_i = 1/2 \cdot I^2 R_{sh}$. Evaluation of I_i in this way does not involve uncertain photometric measurements of sheath width (note that capacitive and visual sheath widths are not equal), nor uses the dc sheath collisionless or highly collisional formulae for evaluation of the slightly collisional RF sheath which usually occurs in experiments. Examples of such a calculation of the ion current are given in Fig. 20 for different gas pressures, together with directly measured ion currents to RF electrodes [15]. The comparison of I_i values obtained by the two independent methods demonstrates better than expected agreement.

IV. Concluding Remarks

The electrical characteristics of symmetrically driven 13.56 MHz RF discharges in argon have been measured with high accuracy and reliability in a specially designed experiment that provides a well-defined discharge along with the simplest possible geometry. The measurements given here cover a comprehensive range of discharge parameters and are suitable for comparison with existing models and for verification of scaling laws based on generally accepted concepts.

Over a wide range of parameters the current/voltage characteristics of the RF discharge in argon were found to be close to linear, as previously observed for the RF discharge in helium and mercury. This seems to contradict the concept of an RF sheath based on Child–Langmuir law or its collisional analog. Moreover, as shown here, the commonly used relationship $V_{dc} \propto V_{sh} = V$ is fulfilled only at very high discharge voltages (higher than or near the upper limit of voltages encountered in applications).

Detailed comparisons of existing RF sheath models with experiments deserve separate consideration and will be addressed in a forthcoming paper. Probe measurements of the electron energy distribution and plasma density carried out for the conditions of the present work have already been preliminarily reported [31], [40], and detailed results of these measurements will soon be published elsewhere.

Acknowledgment

The authors would like to acknowledge J. M. Proud and J. Gustafson for their support and encouragement of this work.

References

[1] J. S. Logan, N. M. Mazza, and P. D. Davidse, "Electrical characterization of radio-frequency sputtering gas discharge," *J. Vac. Sci. Technol.*, vol. 6, p. 120, 1969.

[2] J. W. Coburn, "A system for determining the mass and energy of particles incident on a substrate in a planar diode sputtering system," *Rev. Sci. Instrum.*, vol. 41, p. 1219, 1970.

[3] D. L. Flamm, "A model and apparatus for electrical discharge experiments," *Ind. Eng. Chem. Fund.*, vol. 14, p. 263, 1975.

[4] J. H. Keller and W. B. Pennebaker, "Electrical properties of RF sputtering systems," *IBM J. Res. Rev.*, vol. 23, p. 3, 1979.

[5] A. J. van Roosmalen, "Plasma parameter estimation from RF impedance measurements in a dry etching system," *Appl. Phys. Lett.*, vol. 42, p. 416, 1983.

[6] A. J. van Roosmalen, W. G. M. van den Hoek, and H. Kalter, "Electrical properties of planar RF discharges for dry etching," *J. Appl. Phys.*, vol. 58, p. 653, 1985.

[7] P. Bletzinger and M. J. Flemming, "Impedance characteristics of an RF parallel plate discharge and the validity of a simple circuit model," *J. Appl. Phys.*, vol. 62, p. 4688, 1989.
[8] B. Andries, G. Ravel, and L. Peccoud, "Electrical characterization of radio-frequency parallel-plate capacitively coupled discharges," *J. Vac. Sci. Technol.*, vol. A7, p. 2774, 1989.
[9] J. W. Butterbaugh, L. D. Baston, and H. H. Sawin, "Measurement and analysis of radio frequency glow discharge electrical impedance and network power loss," *J. Vac. Sci. Technol.*, vol. A8, p. 916, 1990.
[10] C. Beneking, "Power dissipation in capacitively coupled RF discharges," *J. Appl. Phys.*, vol. 68, p. 4461, 1990.
[11] V. A. Godyak, R. B. Piejak, and B. M. Alexandrovich, "An experimental system for symmetric capacitive RF discharge studies," *Rev. Sci. Instrum.*, vol. 61, p. 2401, 1990.
[12] V. A. Godyak and R. B. Piejak, "*In situ* simultaneous radio frequency discharge power measurements," *J. Vac Sci. Technol.*, vol. A8, p. 3833, 1990.
[13] V. A. Godyak and R. B. Piejak, "Abnormally low electron energy and heating-mode transition in a low-pressure argon RF discharge a 13.56 MHz," *Phys. Rev. Lett.*, vol. 65, p. 996, 1990.
[14] V. A. Godyak and R. B. Piejak, "Probe measurements of the space potential in a radio frequency discharge," *J. Appl. Phys.*, vol. 68, p. 3157, 1990.
[15] V. A. Godyak, R. B. Piejak, and B. M. Alexandrovich, "Ion flux and ion power losses at the electrode sheaths in a symmetrical RF discharge," *J. Appl. Phys.*, vol. 69, p. 3455, 1991.
[16] V. A. Godyak, O. A. Popov, and A. H. Hanna, "Effective electron collision frequency in RF discharge," *Fiz. Plazmy*, vol. 2, p. 1010, 1976 (also in, *Sov. J. Plasma Phys.*, vol. 2, p. 560, 1976).
[17] A. Popov and V. A. Godyak, "Power dissipated in low pressure RF discharge plasmas," *J. Appl. Phys.*, vol. 57, p. 53, 1986.
[18] V. A. Godyak and A. H. Hanna, "Collisional RF discharge," *Fiz. Plazmy*, vol. 6, p. 676, 1980 (also in, *Sov. J. Plasma Phys.*, vol. 6, p. 372, 1980).
[19] V. A. Godyak, "Steady-state RF discharges at low pressure," *Fiz. Plasmy*, vol. 2, p. 141, 1976 (also in, *Sov. J. Plasma Phys.*, vol. 2, p. 78, 1976).
[20] V. A. Godyak, O. A. Popov, and A. H. Hanna, "Investigation of space charge sheath at electrodes in RF discharge," in *Proc. XIII ICPIG* (Berlin), 1977, P. Bachman and M. Kastelewicz, Eds. Berlin: Phys. Soc. GDR, 1977, p. 347.
[21] V. A. Godyak and N. Sternberg, "Dynamic model of the electrode sheaths in symmetrically driven RF discharges," *Phys. Rev.*, vol. A42, p. 2299, 1990.
[22] V. A. Godyak, *Soviet Radio Frequency Discharge Research*. Falls Church, VA: Delphic Assoc. Inc., 1986, p. 43.
[23] V. A. Godyak, *Soviet Radio Frequency Discharge Research*. Falls Church, VA: Delphic Assoc. Inc., 1986, pp.79–100.
[24] J. Taillet, "Resonance-sustained radio frequency discharges," *J. Phys.*, vol. 37, p. 423, 1969.
[25] V. A. Godyak and O. A. Popov, "Experimental study of resonant RF discharges," *Fiz. Plazmy*, vol. 5, p. 400, 1979 (also in, *Sov. J. Plasma Phys.*, vol. 5, p. 227, 1979).
[26] F. Schneider, "The mechanism of high frequency discharge between level plates," *Z. Angew. Phys.*, vol. 6, p. 456, 1954.
[27] V. A. Godyak, "Statistical heating of electrons at an oscillating plasma boundary," *Zh. Tech. Fiz.*, vol. 16, p. 1364, 1972 (also in, *Sov. Phys. Tech. Phys.*, vol. 16, p. 1073, 1972).
[28] E. Everhart and S. C. Brown, "The admittance of high frequency gas discharges," *Phys. Rev.*, vol. 76, p. 839, 1949.
[29] W. P. Allis, S. C. Brown, and E. Everhart, "Electron density distribution in a high frequency discharge in the presence of plasma resonance," *Phys. Rev.*, vol. 84, p. 519, 1951.
[30] V. A. Godyak and A. H. Hanna, "Influence of self-field on the spatial distribution of a plasma of an RF discharge," *Fiz. Plazmy*, vol. 5, p. 670. 1979 (see also, *Sov. J. Plasma Phys.*, vol. 5, p. 376, 1979).
[31] V. A. Godyak and R. B. Piejak, "A comparison of electron energy distributions in Ar and He RF discharges," in *Proc. XX ICPIG* (Pisa), 1991.
[32] M. A. Lieberman, "Analytical solution for capacitive RF sheath," *IEEE Trans. Plasma Sci.*, vol. 16, p. 638, 1988.
[33] O. A. Popov and V. A. Godyak, "Electron oscillation velocity and electric field in collisionless radio-frequency discharge plasmas," *J. Appl. Phys.*, vol. 59, p. 1759, 1986.
[34] M. Surendra and D. B. Graves, "Particle simulations of radio frequency glow discharges," *IEEE Trans. Plasma Sci.*, vol. 19, p. 144, Apr. 1991.
[35] V. A. Godyak and A. S. Khanneh, "Ion bombardment secondary electron maintenance of steady RF discharge," *IEEE Trans. Plasma Sci.*, vol. PS-14, p. 112, 1986.
[36] V. A. Godyak, *Soviet Radio Frequency Discharge Research*. Falls Church, VA: Delphic Assoc. Inc., 1986, pp. 110–113.
[37] N. Mutsukura, K. Kobayashi, and Y. Mach, "Plasma sheath thickness in radio-frequency discharges," *J. Appl. Phys.*, vol. 68, p. 2657, 1990.
[38] D. Vendor and R. W. Boswell, "Numerical modeling of low-pressure RF plasma," *IEEE Trans. Plasma Sci.*, vol. 18, p. 725, 1990.
[39] M. Lieberman, "Dynamics of a collisional, capacitive RF sheath," *IEEE Trans. Plasma Sci.*, vol. 17, p. 65, 1989.
[40] V. A. Godyak, R. B. Piejak, and B. M. Alexandrovich, "EEDF evolution in low pressure capacitive argon RF discharges at 13.56 MHz," presented at the 43rd Ann. Gas. Elec. Conf.; see also, *Bull. Amer. Phys. Soc.*, vol. 36, p. 207 1991.

Valery A. Godyak (M'91) was born in Czernowitz, USSR, on June 8, 1941. He received the engineer-physicist diploma (an equivalent of the M.S. degree) in physical electronics from the Leningrad Politechnic Institute in 1964, and the Ph.D. degree in plasma physics from Moscow State University in 1968. His Ph.D. thesis was entitled the "Study of RF Field Interaction with Bounded Plasma."

After receiving the engineer-physicist diploma in 1964, he was an Assistant Professor of Physics at the Ryazan Radiotechnic Institute, Ryazan, USSR. In 1968 he joined the Laboratory of Fusion Engineering Problems at the Institute of Electro-Physical Apparatus, Leningrad, where he conducted research and development on high-current relativistic electron accelerators, particularly on field emission, electron optic, and the diagnostics of relativistic electron beams. In 1972 he returned to the Physics Department at Moscow State University, where he was involved in the basic research of RF discharges up to his expulsion for political reasons in 1981. After immigrating to the United States in 1984, he joined the GTE Products Corporation, Danvers, MA, and in 1989, GTE Laboratories Incorporated, Waltham, MA. His current research is on RF discharges, including basic research and application to light source technology.

Dr. Godyak is a Fellow of the American Physical Society.

Robert B. Piejak was born in Passaic, NJ, in 1948. He received the B.S. degree in electrical engineering from the University of Delaware in 1970, and the M.S. and Ph.D. degrees in electrical engineering from the University of Arizona in 1973 and 1977, respectively. In his thesis work he studied parametric instabilities in low-pressure plasmas.

Since 1977 he has been with GTE Laboratories Incorporated, Waltham, MA, where he has worked in the Electrical Products Group and the Light Source Technology Group. In the past he has studied arc behavior and motion in circuit breakers and high-pressure diffuse discharges relevant to fast switches. His present research interests are in the study of low-pressure RF discharges and their application to light sources.

Benjamin M. Alexandrovich was born in Odessa, USSR, in 1947. He received the B.S. degree in electrical engineering from the Institute of Electronics and Communication in Odessa.

During most of his professional career in the USSR, he worked in the area of measurement instrumentation and precision test equipment. He joined GTE Laboratories Incorporated in 1989. Since then, he has been working on electrical measurements and diagnostics of RF discharges.